DTU Library

Active Warping Control For Damping Of Torsional Beam Vibrations

Hoffmeyer, David; Høgsberg, Jan

Published in:
Proceedings of the 9th Conference on Smart Structures and Materials SMART 2019

Publication date:
2019

Document Version
Publisher's PDF, also known as Version of record

Citation (APA):
Hoffmeyer, D., & Høgsberg, J. (2019). Active Warping Control For Damping Of Torsional Beam Vibrations. In A. Benjeddou, N. Mechbal, & J. F. Deü (Eds.), *Proceedings of the 9th Conference on Smart Structures and Materials SMART 2019* (pp. 158-168). International Center for Numerical Methods in Engineering.

IX ECCOMAS Thematic Conference on Smart Structures and Materials
SMART 2019
A. Benjeddou, N. Mechbal and J.F. Deü (Eds)

ACTIVE WARPING CONTROL FOR DAMPING OF TORSIONAL BEAM VIBRATIONS

David Hoffmeyer* **& Jan Høgsberg**

Department of Mechanical Engineering, Technical University of Denmark
Nils Koppels Allé, building 404, DK-2800 Kongens Lyngby, Denmark
e-mail: davhoff@mek.dtu.dk, jhg@mek.dtu.dk, www.dtu.dk

Key words: Torsional beam vibrations, structural dynamics, warping, active control, position feedback, finite element method.

Abstract. This paper considers damping of torsional beam vibrations by active control of the axial warping displacements. A beam element with active positive position feedback (PPF) is set up with an additional flexibility parameter. This arises from partial restraining of warping caused by discrete actuators. The flexibility lowers the frequency associated with an infinite actuator gain and thereby the attainable damping ratio. It is shown how it furthermore affects the stability limit. Results are compared with three-dimensional finite element results, with multiple actuators acting on an end cross-section of the beam. The accuracy of the beam model is justified by an example which shows that substantial damping ratios may be achieved by active warping control.

1 INTRODUCTION

Slender structures like long bridge decks, aircraft wings, wind turbine blades and general thin-walled beams may be prone to vibrations due to loads like wind, traffic etc. If the loads act with an eccentricity relative to the shear center or if the cross-section lacks double symmetry, torsional vibrations may be induced. For some structures the aerodynamic instability phenomenon flutter may occur where flexural and torsional vibrations couple. To potentially avoid flutter or to reduce fatigue stresses, structural mass or accelerations, supplemental damping may be required.
Torsion of thin-walled beams generates out-of-plane, axial warping displacements that are often significant at the boundaries of beams with open cross-sections. Thus, for these types of thin-walled beams the restraining of warping results in an often considerable increase in the natural frequency and change in vibration characteristics as described by Gere [1]. The localized effect of restrained warping is used in [2] to introduce a substantial amount of supplemental damping by applying an energy dissipating boundary condition. In [3] discrete viscous dampers constituting a pure bimoment are placed on the beam cross-section of a three-dimensional finite element model, showing convincing agreement with the governing transcendental equation.

For beams with closed cross-sections or when torsion couples with flexure, viscous dampers may not be sufficient or even practically applicable. Thus, in the present work an active damping concept is used for damping of pure torsional vibrations. A positive position feedback (PPF) [4] signal is passed by a sensor through a simple linear filter to an actuator which produces an active force. The damping

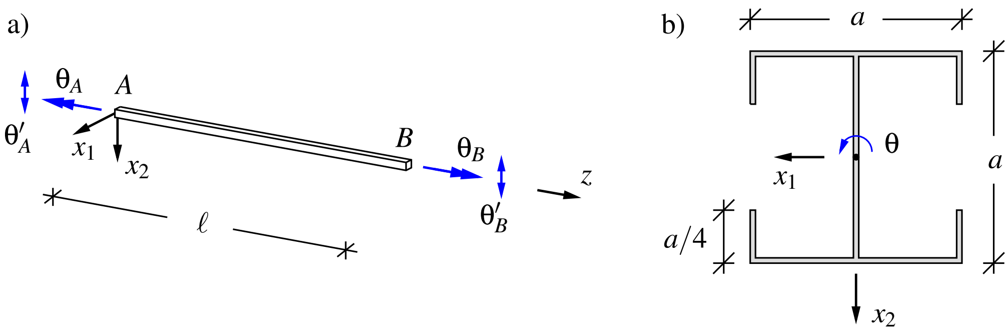

Figure 1: a) beam with degrees-of-freedom and b) thin-walled cross-section with coordinate system.

concept is applied with a beam element and compared with a full three-dimensional finite element (FE) analysis. In an actual structure the actuators are placed as discrete actuators on a beam cross-section, thus only partially restraining the warping. This is associated with an additional flexibility that lowers the frequency obtained when the actuators completely lock - which in control theory typically is refered to as a zero - and thereby also the maximum damping ratio determined as the relative imaginary part of the natural frequency. This flexibility is incorporated into the beam element as a Maxwell-type boundary condition, and is calibrated by dedicated finite element results. The system is solved in state-space form and it is shown that substantial damping ratios may be obtained for the lowest torsional mode. For the position feedback the control gain is limited by stability yielding a gain as derived in [5]. At a certain point the actuator will eliminate the structural stiffness at the location of the actuator and the response becomes unbounded. This limit, however, is based on a static condition and it is shown how the additional flexibility from restraining warping partially affects this limit.

2 STRUCTURAL EQUATIONS

In this section the governing structural equations are presented. First the differential equation governing pure torsion is presented and then the beam is discretized with beam elements, resulting in the governing multi-degree-of-freedom equations.

2.1 Uncoupled torsional vibrations

Consider the beam in Fig. 1a with length ℓ, longitudinal axis z and transverse axes $\{x_1,x_2\}$. For a cross-section like the one in Fig. 1b with double symmetry, the elastic and shear centers coincide and the torsional and flexural vibrations thereby uncouple. The rotation with respect to the shear center is denoted $\theta(t,z)$ and the warping intensity is the spatial derivative of the rotation $\theta'(t,z)$. The differential equation governing pure torsional vibrations may be derived as [1, 3, 6],

$$EI_\psi\theta''''(t,z) - GK\theta''(t,z) - \rho I_\psi\ddot{\theta}''(t,z) + \rho J\ddot{\theta}(t,z) = 0 \tag{1}$$

where E is Young's modulus, G is the shear modulus, ρ is the mass density, I_ψ is the warping moment of inertia, K is the torsion stiffness parameter, $()' = \partial()/\partial z$ denotes partial differentiation with respect to z and $\dot{()} = \partial()/\partial t$ denotes partial differentiation with respect to t. The third term is the inertia associated with the axial warping [6] and is often neglected due to its limited importance.

2.2 Discretization with beam elements

The torsion problem is now implemented in a finite element setting and the structure is discretized with beam elements. As pure torsional vibrations are considered the beam element only contains the two torsional degrees-of-freedom as depicted in Fig. 1a, that is the rotation and warping intensity. The four degrees-of-freedom for the beam element are interpolated as,

$$\theta = \mathbf{N}\left[\theta_A\,,\,\ell\theta'_A\,,\,\theta_B\,,\,\ell\theta'_B\right]^T \tag{2}$$

where the displacement interpolation array $\mathbf{N}$ contains the Hermitian shape functions,

$$\mathbf{N} = \left[2s^3 - 3s^2 + 1\;,\; s(s-1)^2\;,\; -2s^3 + 3s^2\;,\; s^2(s-1)\right] \tag{3}$$

where $s = z/\ell$ is a local element coordinate. The element stiffness matrix $\mathbf{K}$ and mass matrix $\mathbf{M}$ are associated with the elastic and kinetic energy respectively. Setting up the energies and assuming a prismatic beam element leads to the explicit expression for the stiffness matrix

$$\mathbf{K} = EI_\psi \ell^{-3}\begin{bmatrix} 12 & & & \\ 6 & 4 & & \\ -12 & -6 & 12 & \\ 6 & 2 & -6 & 4 \end{bmatrix} + GK\ell^{-1}\frac{1}{30}\begin{bmatrix} 36 & & & \\ 3 & 4 & & \\ -36 & -3 & 36 & \\ 3 & -1 & -3 & 4 \end{bmatrix} \tag{4}$$

with contributions from homogeneous and inhomogeneous torsion through GK and EI_ψ respectively. The mass matrix takes a similar form,

$$\mathbf{M} = \rho J\ell\frac{1}{420}\begin{bmatrix} 156 & & & \\ 22 & 42 & & \\ 54 & 13 & 156 & \\ -13 & -3 & -22 & 4 \end{bmatrix} + \rho I_\psi \ell^{-1}\frac{1}{30}\begin{bmatrix} 36 & & & \\ 3 & 4 & & \\ -36 & -3 & 36 & \\ 3 & -1 & -3 & 4 \end{bmatrix} \tag{5}$$

The first term in (5) contains the torsional inertia and the second term contains the warping inertia. The latter is usually of limited importance and often discarded but may in this format easily be implemented through the submatrices. The local elements are easily assembled and transformed to a global structure [7].

2.3 Multi-degree-of-freedom system

As the model is discretized with beam elements the equations of motion are given in terms of the displacement vector $\mathbf{q}(t)$ of the linear system and the corresponding stiffness matrix $\mathbf{K}$ and mass matrix $\mathbf{M}$ from Section 2.2. Neglecting any inherent structural damping the system has the general form,

$$\mathbf{M}\ddot{\mathbf{q}}(t) + \mathbf{K}\mathbf{q}(t) = -\mathbf{w}B_d(t) \tag{6}$$

where $B_d(t)$ represents the effect of the external actuator on the system in the form of a bimoment [6]. The corresponding connectivity vector $\mathbf{w}$ identifies the point on the structure connected to the actuator for the beam with a single actuator. The vector has the structure $\mathbf{w} = [0,...,1,...,0]^T$ with the single entry defining the degree-of-freedom associated with the actuator.
The actuator is assumed linear and collocated and may be formulated by a frequency transfer function $H(\omega)$ and gain g in the form

$$B_d(t) = gH(\omega)\mathbf{w}^T\mathbf{q}(t) \tag{7}$$

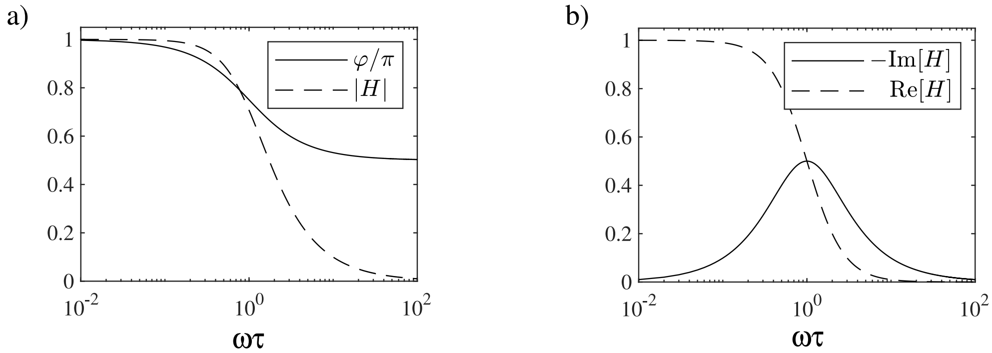

Figure 2: a) magnitude and phase angle and b) real and imaginary part of the transfer function $H(\omega)$.

The frequency function may take several different forms based on the particular control law. By introducing (7) in (6) the equations of motion may be written in the frequency domain as

$$\left(-\omega_n^2\mathbf{M}+\mathbf{K}+gH(\omega)\mathbf{w}\mathbf{w}^T\right)\widetilde{\mathbf{q}}_n=\mathbf{0} \tag{8}$$

where $\widetilde{()}$ indicates the amplitude. If $g=0$ the actuator does not influence the structure and the solution to the eigenvalue problem in (8) will give real-valued solutions in form of the undamped natural frequencies $\omega_{0,n}$. If, on the other hand, $g\to\infty$ the actuator will lock and prohibit displacement at its location, whereby the solution to the eigenvalue problem provides the infinitely damped frequencies $\omega_{\infty,n}$, associated with infinite gain. The frequencies ω_0 and ω_∞ are typically denoted pole and zero respectively within control theory.

3 Active control by position feedback

Active control is now introduced by a positive position feedback. The control system detects the axial warping displacement at the end cross-section during the torsional motion, passes it through a simple linear first order filter and feeds it positively back to the structure. The position feedback is deemed appropriate as the warping displacements are small and easily measured by e.g. a piezoelectric sensor or a laser device. The filter is mathematically formulated as [8]

$$B_d(t)+\tau\dot{B}_d(t)=g\theta_g'(t) \tag{9}$$

where $\theta_g'=\mathbf{w}^T\mathbf{q}$ is the displacement at the actuator which in this case constitutes the warping intensity, B_d is the actuator force constituting a bimoment which is energy conjugate to the warping intensity and τ is a filter constant which defines the cut-off frequency at $1/\tau$. Based on the displacement $\theta_g'(t)$ the equivalent actuator force $B_d(t)$ is fed back to the system. The transfer function for the filter in (9) is hereby obtained as

$$gH(\omega)=\frac{g}{1+i\omega\tau} \tag{10}$$

The corresponding phase angle and magnitude are determined as

$$\tan\varphi=-\omega\tau \qquad , \qquad |H|=\frac{1}{\sqrt{1+(\omega\tau)^2}} \tag{11}$$

The phase angle and magnitude are seen in Fig. 2a. This specific filter ensures large damping in the low-frequency range below the cut-off frequency, while attenuating noisy high-frequency components

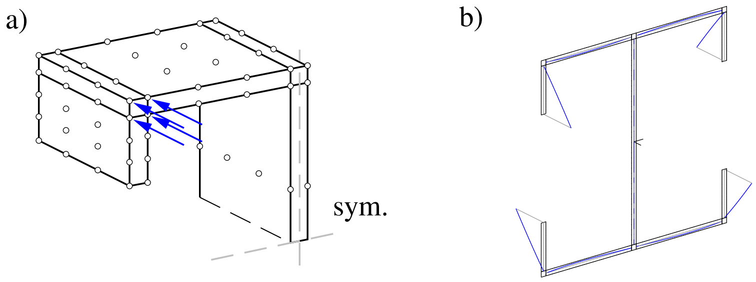

Figure 3: a) quarter cross-section discretized with isoparametric elements and with local actuators and b) altered cross-sectional warping.

which may be badly represented. By the punctured curve in Fig. 2a it is evident that this is achieved as the magnitude of the transfer function vanishes above the cut-off frequency. The major benefit of active control is the possibility of greater damping performance when the actuator leads velocity with a phase angle $\varphi > \pi/2$. Especially in the low-frequency range this filter exhibits a phase angle close to π as indicated by the solid curve, and therefore has a force component in phase with negative stiffness.
In order for the actuator to dissipate energy and not amplify the vibrations, it is required that $\mathrm{Im}[gH(\omega)] > 0$. In Fig. 2b the solid curve represent the imaginary part of the transfer function. As this is negative, it means that $g < 0$.

3.1 Warping-restrained flexibility

In practice warping control may be realized by axial actuators, acting on the cross-section as shown in Fig. 3a. In a situation with concentrated axial actuators applied at a cross-section the actuators will only fully restrain the warping displacements at the location of the actuators. At infinitely high gain, i.e. when $g \to \infty$, the axial movement at the actuator location will be completely prevented. However, the cross-section may still able to warp in between the actuators and leave an altered warping function as illustrated in Fig. 3b. This is associated with an additional flexibility compared to a fully restrained cross-section [3]. At vanishing damping ($g = 0$) the additional flexibility must however disappear. This additional flexibility may therefore be modelled as a spring in series with the actuator, as seen in Fig. 4. The warping works through the gradient of the angle of twist and therefore so does the spring. It is, however, an artificial spring as it is not physically present, but merely describes the additional flexibility due to the partial warping of the cross-section for $g > 0$. Thereby it may conveniently be modelled as a Maxwell-type boundary condition. The total gradient of the angle of twist, θ'_d, is the sum of the contribution from the actuator and spring as seen in Fig. 4,

$$\theta'_d(t) = \theta'_k(t) + \theta'_g(t) \tag{12}$$

where it works through the actuator bimoment B_d. The bimoment produced by the spring is

$$B_k(t) = k\theta'_k(t) \tag{13}$$

and the bimoment produced by the actuator is given by (9). Introducing (9) and (13) into (12) yields the modified control equation, to be used for calibration of g and identification of the stability limit,

$$\left(\frac{1}{g} + \frac{1}{k}\right) B_d(t) + \frac{\tau}{g}\dot{B}_d(t) = \theta'_d(t) \tag{14}$$

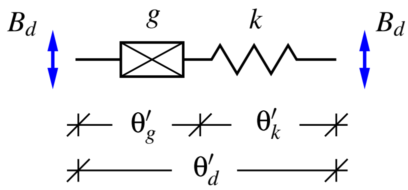

Figure 4: Maxwell-type boundary condition with an active element with gain g in series with a spring with stiffness k.

The determination of k requires in this case knowledge about the actual structure either from a full three-dimensional finite element model, from experiments or from real measurements. The stiffness k in the flexibility format reduces the infinitely damped frequency ω_∞ as the cross-section is now able to warp in between the actuator locations. However, due to the active nature of the actuator there will be a stability limit, see Section 3.3, where the response becomes unbounded. In the complex plane, however, the root locus will trace towards the correct infinitely damped frequency, as the controller equation (14) in the limit describes only the additional flexibility,

$$\left(\frac{1}{g}+\frac{1}{k}\right)B_d(t)+\frac{\tau}{g}\dot{B}_d(t)=\theta'_d \quad \rightarrow \quad B_d(t)=k\theta'_d \qquad \text{for} \quad g\rightarrow\infty \tag{15}$$

This means that the structural equations are merely supplemented with a spring, incorporated in flexibility format, when establishing the state-space equations in the following section. The stiffness k is calibrated in the unstable situation where $g \rightarrow \infty$, but this is equivalent with a situation where the actuators are replaced with supports and may thus be used for calibration.

3.2 State-space formulation

The properties of the dynamic system with damping is conveniently demonstrated in the frequency domain. The equations of motion are therefore set up in a state-space format including the feedback force from (14). With the state-vector $\mathbf{z}(t) = [\mathbf{q}(t)\,,\dot{\mathbf{q}}(t)\,,B_d(t)]^T$ the system is

$$\frac{d}{dt}\begin{bmatrix}\mathbf{q}(t)\\ \dot{\mathbf{q}}(t)\\ B_d(t)\end{bmatrix}=\begin{bmatrix}\mathbf{0} & \mathbf{I} & \mathbf{0}\\ -\mathbf{M}^{-1}\mathbf{K} & \mathbf{0} & -\mathbf{M}^{-1}\mathbf{w}\\ g/\tau\mathbf{w}^T & \mathbf{0} & -g/\tau\left(\frac{1}{g}+\frac{1}{k}\right)\end{bmatrix}\begin{bmatrix}\mathbf{q}(t)\\ \dot{\mathbf{q}}(t)\\ B_d(t)\end{bmatrix} \tag{16}$$

where $\mathbf{I}$ is the identity matrix. The presence of the actuator leads to generally complex-valued solutions of ω,

$$\omega_n = |\omega_n|\left(\sqrt{1-\zeta_n^2}+i\zeta_n\right) \tag{17}$$

where n denotes the various eigensolutions. The damping ratio is given by the imaginary part of (17) as

$$\zeta_n = \frac{\mathrm{Im}[\omega_n]}{|\omega_n|} \tag{18}$$

The mode shapes obtained from (16) are in general also complex, with the real part representing the physical vibration form and the imaginary part representing the spatial phase shift due to the presence of the energy dissipating actuator.

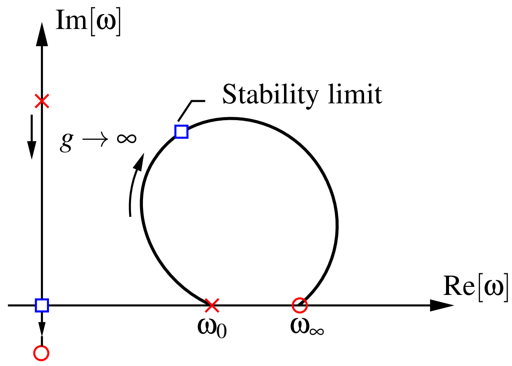

Figure 5: Root locus and indication of the stability limit when the purely imaginary eigenvalue becomes negative.

3.3 Stability and gain limit

When solving (16) varying the gain in the interval $g \in [0; \infty[$ the damped frequency will trace a root locus in the complex plane between the undamped frequency ω_0 and the infinitely damped frequency ω_∞ as shown in Fig. 5. However, as mentioned in Section 3.1 after a certain gain the response becomes unbounded. With a single actuator present, a single eigenvalue will be purely imaginary. Instability occurs when this eigenvalue becomes zero. In order for the response not to become unbounded the stability of the system must therefore be considered. This is mainly to set a limit for the gain g. The stability of the system may be checked with the Routh-Hurwitz criterion. For larger systems this typically requires determination of the Routh arrays and may not be convenient to determine an explicit limit for the gain. An alternative is to write the full system consisting of the structural equations (6) and the controller equation (14) in a block format. The structural equations and controller equation are pre-multiplied with $-g\nu^{-1}$ where $\nu = \left(1 + \frac{g}{k}\right)$, and the original structural displacement vector $\mathbf{q}$ is replaced by the modified set of variables in $\mathbf{q}^* = -g\nu^{-1}\mathbf{q}$. The equations then take the form

$$\begin{bmatrix} \mathbf{M} & \mathbf{0} \\ \mathbf{0} & 0 \end{bmatrix} \begin{bmatrix} \ddot{\mathbf{q}}^* \\ \ddot{B}_d \end{bmatrix} + \begin{bmatrix} \mathbf{C} & \mathbf{0} \\ \mathbf{0} & -g\nu^{-2}\tau \end{bmatrix} \begin{bmatrix} \dot{\mathbf{q}}^* \\ \dot{B}_d \end{bmatrix} + \begin{bmatrix} \mathbf{K} & -g\nu^{-1}\mathbf{w} \\ -g\nu^{-1}\mathbf{w}^T & -g\nu^{-1} \end{bmatrix} \begin{bmatrix} \mathbf{q}^* \\ B_d \end{bmatrix} = \begin{bmatrix} \mathbf{0} \\ 0 \end{bmatrix} \tag{19}$$

It is noted that if $|g| < k$ then $\nu > 0$. The mechanical energy is defined by the first and last matrix. The equivalent mass matrix is always positive semi-definite, and as $\tau > 0$ the equivalent damping matrix will be positive definite if the original structure has positive definite damping and is otherwise positive semi-definite. The stability is therefore entirely governed by the equivalent stiffness matrix and the corresponding reduction in stiffness caused by the actuator with the added warping-restrained flexibility. The potential energy associated with the stiffness matrix can be expressed as

$$V_e = \begin{bmatrix} \mathbf{q}^{*T} & B_d \end{bmatrix} \begin{bmatrix} \mathbf{K} & -g\nu^{-1}\mathbf{w} \\ -g\nu^{-1}\mathbf{w}^T & -g\nu^{-1} \end{bmatrix} \begin{bmatrix} \mathbf{q}^* \\ B_d \end{bmatrix} \tag{20}$$

After some rearranging it takes the form

$$\begin{aligned} V_e = \tfrac{1}{2}\mathbf{q}^{*T}\left[\mathbf{K} + g\nu^{-1}\mathbf{w}\mathbf{w}^T\right]\mathbf{q}^* + \tfrac{1}{2}\Big(B_d\left(g\nu^{-1}\right)^{1/2} - \left(g\nu^{-1}\right)^{1/2}\mathbf{w}^T\mathbf{q}^*\Big)^2 \\ - B_d g\nu^{-1}B_d - \mathbf{q}^{*T}g\nu^{-1}\mathbf{q}^* \end{aligned} \tag{21}$$

The time derivative of this functional is given by the second matrix in (19) as

$$\dot{V}_e = -\left[\dot{\mathbf{q}}^{*T}\mathbf{C}\dot{\mathbf{q}}^{*} - \dot{B}_d g \nu^{-2} \tau \dot{B}_d\right] \leq 0 \tag{22}$$

The second term in (21) is a quadratic form and thus always positive, while the third and fourth terms are also positive as $g < 0$. Stability is therefore governed by the first term of which the matrix must be positive definite for the combined system to be stable. If the matrix becomes singular it corresponds to the stiffness component of the actuator eliminating the structural stiffness at the location of the actuator and instability occurs. This corresponds to the requirement

$$\det\left(\mathbf{K} + g\nu^{-1}\mathbf{w}\mathbf{w}^T\right) > 0 \tag{23}$$

Thus the matrix in the parentheses must be invertible and the limit of the gain, g_{stab}, may be found by considering the invertibility of the matrix. The result follows from the Sherman-Morrison formula [9] as

$$\left(\mathbf{K} + g\nu^{-1}\mathbf{w}\mathbf{w}^T\right)^{-1} = \mathbf{K}^{-1} - g\nu^{-1}\mathbf{K}^{-1}\mathbf{w}\left(1 + g\nu^{-1}\mathbf{w}^T\mathbf{K}^{-1}\mathbf{w}\right)^{-1}\mathbf{w}^T\mathbf{K}^{-1} \tag{24}$$

When rigid body motion is accounted for, the stiffness matrix will be fully positive definite. Thus, if the term in the parenthesis on the right side of (24) becomes zero, the term may not be inverted. This determines the gain limit as

$$\frac{1}{g_{\text{stab}}} = -\mathbf{w}^T\mathbf{K}^{-1}\mathbf{w} - \frac{1}{k} \tag{25}$$

The above expression leaves a direct way of determining the maximum gain, which is at the same time seen to be negative. A gain that exceeds the above limit will result in an unbounded response.

4 Comparison with a 3D FEM model

The beam model is compared with a full three-dimensional FE model with isoparametric elements. The elements used are bi-cubic-linear elements for flange parts and bi-linear-cubic elements for corners and junctions. For details on the elements and discretization of the beam see [3]. The beam is discretized with 30 length-wise elements, half of them being concentrated over $\ell/25$ of the beam near the end, and a single bi-cubic-linear element per flange part as in Fig. 3a. In the three-dimensional model, actuators are applied in the corners as in Fig. 3a, and as they are placed asymmetrically they are balanced according to [3, 10]. Thus, m actuators are present and the feedback filter now contains several equations written in vector format as

$$\mathbf{f}_d + \tau\dot{\mathbf{f}}_d = \mathbf{G}\mathbf{W}^T\mathbf{q} \tag{26}$$

This equation resembles (9) but without the flexibility k. In order not to damp other modes than those associated with torsion, each connectivity vector $\mathbf{w}_j$ contains contributions from exactly four actuators constituting a pure bimoment. These four actuators are placed symmetrically in the corners with respect to the principal axes of the cross-section in Fig. 1, and thus only one of the four actuators in each corner as indicated in Fig. 6b enters each connectivity vector. Thus the structure is $\mathbf{w}_j = [0, \ldots, -\sqrt{1/4}, \sqrt{1/4}, -\sqrt{1/4}, \sqrt{1/4}, \ldots, 0]^T$. The collective array $\mathbf{W} = [\mathbf{w}_1, \mathbf{w}_2, \ldots, \mathbf{w}_{m/4}]$ contains $m/4$ connectivity vectors and $\mathbf{G} = \mathrm{diag}[g_1, g_2, \ldots, g_{m/4}] = g^{3\mathrm{D}}\,\mathrm{diag}[\alpha_1, \alpha_2, \ldots, \alpha_{m/4}]$ is a diagonal matrix with all gains. The actuators are in this case not balanced equally due to the asymmetric location of the actuators in Fig. 6. Balancing factors α_j are therefore introduced according to [3] and $g^{3\mathrm{D}}$ is a common gain. The stability requirement is derived in the same way as for the beam model with

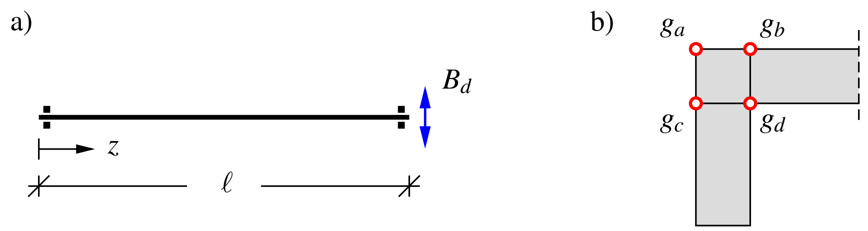

Figure 6: a) 'simple-simple' beam with damping treatment at $z=\ell$ and b) order of actuator gains at cross-section corner.

a single actuator, but the final condition is not an explicit expression for the gain. The following matrix may be derived,

$$\mathbf{H} = \mathbf{G}^{-1} + \mathbf{W}^T\mathbf{K}^{-1}\mathbf{W} \tag{27}$$

which is $m/4 \times m/4$ and will be negative definite for small values of $g^{3\mathrm{D}}$ and thereby have all negative eigenvalues $\lambda_i < 0$. Instability occurs exactly when the first eigenvalue of $\mathbf{H}$ becomes positive. As the beam model and three-dimensional model are inherently different, the gain at instability will not be the same as the actuators are tuned differently. However, by setting up the virtual work produced by the actuator in the beam model and the actuators in the three-dimensional model, a convertion factor can be derived as

$$g^{3\mathrm{D}} = \frac{g}{\sum_j^m \alpha_j \psi_j^2} \tag{28}$$

where ψ_j is the sector-coordinate of the j'th actuator. In the next section it will be shown that instability occurs at the same frequency and damping ratio in the two models.

5 Damping of a 'simple-simple' beam

The accuracy of the beam model is now demonstrated by investigating the damping properties of the lowest torsional mode of the 'simple-simple' beam with length ℓ as shown in Fig. 6a. The support conditions restrain rotation but allow warping. The cross-section of the beam is shown in Fig. 1 and has thickness $t = a/40$, Young's modulus $E = 210$ GPa, Poisson's ratio $\nu = 0.3$ and density $\rho = 7850$ kg/m^3. The ratio between the cross-section height and the length of the beam is $\ell/a = 30$ and $a = 1$ m, for which the inherent distortion of the cross-section is minimal [3]. The beam model is compared with results from a three-dimensional finite element analysis. In this finite element model four actuators are placed at each corner as shown for a single corner in Fig. 6b, and balanced according to Table 1. This is done in order to avoid unnecessary distortion of the cross-section. For the beam model the first objective is to adjust the infinitely damped frequency ω_∞ to account for the partial restrainment of the warping at $z=\ell$. This is done by performing a real analysis of the 3D FE model by solving the full system in (16) with $g \to \infty$ and afterwards calibrating the flexibility parameter k by a numerical search routine to ensure that the frequency locus terminates at the correct frequency. To create the root locus the gain is varied in the interval $g \in [0; g_{\mathrm{stab}}[$ where the stability limit is given by (25) or (27) for the beam and 3D model respectively.

The root loci for both models are seen in Fig. 7a. The solid line with black circles (—,○) are results from the beam model, the red markers (+) are results from the 3D model and the blue box marker (□) indicates the stability limits. Furthermore, the punctured line indicates results for the beam model with $k = \infty$ associated with complete restrainment of the warping of the entire cross-section. For comparison,

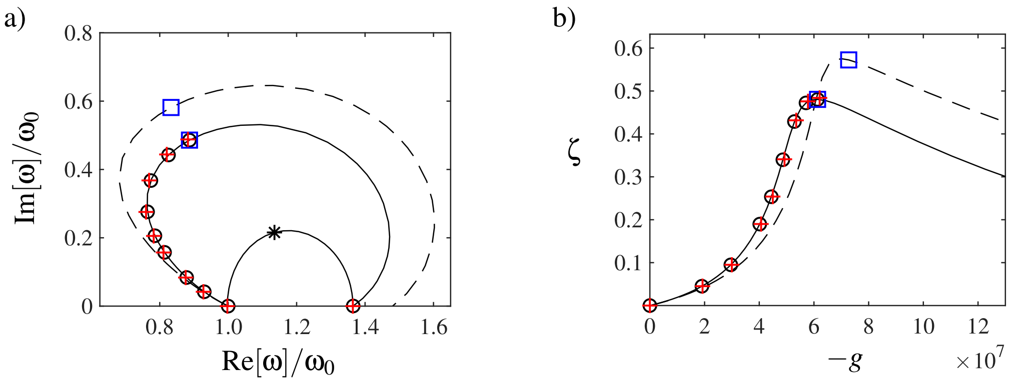

Figure 7: a) root locus and b) damping ratio for the beam analysis (—,○), FE analysis (+), gain limit (□) and $k = \infty$ (– –).

the smaller half-circular root locus is with pure viscous damping, and the asterix (∗) indicates optimal tuning. Clearly the partial restrainment of the warping associated with the flexibility parameter k given in Table 2 results in a significant difference, lowering the relative frequency increment $(\omega_\infty - \omega_0)/\omega_0$ from 0.481 to 0.365 and the damping ratio at instability from 0.572 to 0.480 for the beam model. The damping ratio as may be seen in Fig. 7b also indicates large damping. The damping ratios at instability and the frequency increments for the two models are very similar as seen in the table, and the small deviation is due to distortional effects in the 3D model, which causes slightly different undamped frequencies ω_0. Due to the different nature of the two models and actuator configurations, the limit gains g_{stab} and $g_{\text{stab}}^{\text{3D}}$ are not identical. The factor between these two is $g_{\text{stab}}/g_{\text{stab}}^{\text{3D}} = 50.4$ as seen in the table, and this is approximated well with (28) as seen in the last column in the table. Lastly it may be observed that the gain limit for the beam model is higher if not taking the partial warping restraining into account. This may wrongfully lead to instability.

6 CONCLUSION

In this paper a computationally efficient way of investigating the properties of damping the torsional vibrations in a simple beam with active control is considered. A beam element is set up with a single actuator acting on the warping degree-of-freedom. The actuator consists of a simple linear filter in the form of positive position feedback (PPF). It acts on the axial warping displacements, and is on an actual structure placed discretely as a set of actuators constituting a pure bimoment. This partially restrains the warping and allows for an additional flexibility in the beam model. This flexibility lowers the infinitely damped frequency and correspondingly reduces the gain limit at the point of instability. The beam model is compared with a full three-dimensional finite element model which has a set of actuators applied at discrete locations, all constituting pure bimoments. In this way only torsional modes are damped. The system equations are similar to the beam model, and instability is determined by the gain which makes the combined stiffness matrix singular. Considering a simple-simple beam as an example and plotting the root loci and damping ratios, very similar results between the two models are obtained. Only minor

Table 1: Balancing factors.

	g_a	g_b	g_c	g_d
α_j [−]	1.0	7.5	70.0	141.4

Table 2: Results of analysis.

	k	$(\omega_\infty - \omega_0)/\omega_0$	ζ_{stab}	g_{stab}	$g_{\mathrm{stab}}/g_{\mathrm{stab}}^{3D}$	$\sum_j^m \alpha_j \psi_j^2$
Beam model	∞	0.481	0.572	$-7.27 \cdot 10^7$	–	–
	$3.89 \cdot 10^8$	0.365	0.480	$-6.13 \cdot 10^7$	50.4	51.0
3D model	–	0.368	0.484	$-1.22 \cdot 10^6$		

differences are observed, which may be corrected by accounting for the inherent distortion of the three-dimensional model. It is furthermore demonstrated, that the flexibility k is necessary for the beam model to reflect the 3D model. If not included, a gain exceeding the gain limit may wrongfully be chosen. The gain at instability is inherently different in the two models, but may easily be estimated considering the position of the discrete actuators. The benefits with the active filter is clear, as the beam is damped effectively, with a damping ratio of almost $\zeta = 0.5$.

REFERENCES

[1] Gere, J. M., *Torsional vibrations of Beams of Thin–Walled Open Section*, ASME Journal of Applied Mechanics (1954), vol. 21, no. 4, pp. 381-387.

[2] Høgsberg, J. & Hoffmeyer, D., *Damping of torsional beam vibrations by control of warping displacement*, Journal of Vibration and Acoustics (2016), vol. 138, DOI: 10.1115/1.4031616.

[3] Hoffmeyer, D. & Høgsberg, J., *Damping of torsional vibrations in thin-walled beams by viscous bimoments*, Mechanics of Advanced Materials and Structures (2019), DOI: 10.1080/15376494.2019.1567885.

[4] Fanson, J. L. & Caughey, T. K., *Positive position feedback control for large space structures*, AIAA Journal (1990), vol. 28, no. 4, DOI: 10.2514/3.10451.

[5] Goh, C. J. & Caughey, T. K., *On the stability problem caused by finite actuator dynamics in the collocated control of large space structures*, International Journal of Control (1985), vol. 41, no. 3, 787-802, DOI: 10.1080/0020718508961163.

[6] Vlasov, V. Z., *Thin–walled Elastic Beams*, (1961) Israel Program for Scientific Translations, Jerusalem.

[7] Cook, R. D. et. al., Concepts and Applications of Finite Element Analysis, *John Wiley and Sons*, (2002).

[8] Høgsberg, J. & Krenk, S., *Linear control strategies for damping of flexible structures*, Journal of Sound and Vibration (2006), 293, pp. 59-77, DOI: 10.1016/j.jsv.2005.09.014.

[9] Krenk, S. & Høgsberg, J., *Equal modal damping design for a family of resonant vibration control formats*, Journal of Vibration and Control (2012), vol. 19, no. 9, pp. 1294-1315, DOI: 10.1177/1077546312446796.

[10] Main, J. A. & Krenk, S., *Efficiency and tuning of viscous dampers on discrete systems*, Journal of Sound and Vibration (2005), **286**, pp. 97-122, DOI: 10.1016/j.jsv.2004.09.022.